Zhu, F. Y. *et al.* (2019). *Géotechnique* **69**, No. 10, 924–931 [https://doi.org/10.1680/jgeot.17.P.273]

TECHNICAL NOTE

Suction caisson foundations for offshore wind energy: cyclic response in sand and sand over clay

FANGYUAN ZHU*, BRITTA BIENEN†, CONLETH O'LOUGHLIN†, MARK JASON CASSIDY† and NEIL MORGAN‡

This technical note considers experimental data on the long-term response of a suction caisson in sand and sand over clay to lateral cyclic loading. Installation of the caisson under suction in a geotechnical centrifuge provides insight into the contribution of this installation process, as well as the effects that soil drainage and consolidation in the clay layer have on the accumulated caisson rotation and change in stiffness. The tests focused on sand over clay, and considered variations in the cyclic load magnitude and symmetry. One-way cyclic loading in sand over clay is seen to result in higher rotation than two-way loading, which contrasts with findings from previous studies in sand. Excess pore pressure dissipation in the clay layer leads to strength increases that stabilise caisson rotation and increase stiffness. The rate of accumulation in caisson rotation is observed to be the same from centrifuge and single gravity tests, while the initial rotation differs with stress level, drainage regime, loading magnitude, soil profile and installation method. The centrifuge tests are considered collectively with equivalent single gravity tests to form a basis for predicting the long-term response of a monopod suction caisson.

KEYWORDS: centrifuge modelling; deformation; offshore engineering; soil/structure interaction; stiffness

INTRODUCTION

Monopod suction caisson foundations for offshore wind turbines are subjected to long-term metocean cyclic loading acting laterally on the superstructure. Owing to the sensitivity of turbines to non-verticality and dynamics (Bhattacharya, 2014), the evolution of foundation rotation and foundation–soil stiffness over the design life needs to be understood. Investigations of long-term cyclic loading of suction caissons have predominantly focused on sand (e.g. Zhu *et al.*, 2013; Cox *et al.*, 2014; Foglia *et al.*, 2014). Limited data are available for sand overlying clay (Zhu *et al.*, 2018). However, dense sand over overconsolidated clay seabeds are prevalent in areas of wind farm development in the North Sea (De Ruiter & Fox, 1975; Bond *et al.*, 1997; BGS, 2002). Zhu *et al.* (2018) provide the only publicly available database to date of caisson response under lateral cyclic loading in sand over clay. These tests were performed over approximately $N = 10^6$ load cycles and were complemented with single-layer sand and single-layer clay experiments. The capacity and rotation response were shown to approach those measured in the sand when the sand–clay interface is located at or beneath the caisson skirt tip, while they differ when the sand layer thickness is approximately half the skirt length ($H_{sand} = 0{\cdot}5L$). These experiments were performed as scaled model tests at single gravity, where the caisson was installed by jacking (as in most experiments), showing trends of rotation accumulation that were consistent across the database and with published research on this topic. Therefore, this note considers centrifuge tests that deal with the remaining knowledge gaps associated with the effects of soil self-weight stresses, suction installation and drainage conditions. Considered collectively with the findings from single gravity tests over one million cycles (Zhu *et al.*, 2018) and confirming the trend of rotation accumulation, a simple calculation method is proposed for predicting suction caisson response to long-term lateral cyclic loading in this database.

Manuscript received 30 October 2017; revised manuscript accepted 4 October 2018. Published online ahead of print 22 November 2018. Discussion on this paper closes on 1 March 2020, for further details see p. ii.

* Centre for Offshore Foundation Systems, The University of Western Australia, Crawley, Perth, WA, Australia (Orcid:0000-0003-4041-0728).
† Centre for Offshore Foundation Systems, The University of Western Australia, Crawley, Perth, WA, Australia.
‡ Lloyd's Register EMEA, Aberdeen, UK.

CENTRIFUGE MODELLING

The experimental details are described by Zhu (2018) and Bienen *et al.* (2017), with only brief descriptions provided here. The centrifuge testing campaign was designed to specifically explore the effects of soil self-weight stresses, suction installation and drainage conditions to complement the long-term cyclic loading tests performed at single gravity (Zhu *et al.*, 2018). These had identified the soil profile of dense sand with a thickness of approximately half a caisson skirt length ($H_{sand} = 0{\cdot}5L$) over overconsolidated clay to differ from stratigraphies with larger sand layer depth. As in the paper by Zhu *et al.* (2018), the caisson aspect ratio of skirt length over diameter in the centrifuge tests was $L/D = 0{\cdot}5$, which is realistic and has been adopted in other suction caisson research (e.g. Zhu *et al.*, 2013). The model caisson (Fig. 1) diameter was $D = 80$ mm, noting that the intention was to examine fundamental behaviour, rather than to model a particular caisson dimension. The load eccentricity $M/HD = 3{\cdot}5$ is also within the range realistic for field conditions (e.g. Cox *et al.*, 2014) and has been chosen to correspond to the value in the single gravity tests of Zhu *et al.* (2018).

The centrifuge tests were conducted in a beam centrifuge at an acceleration of 100$\boldsymbol{g}$. This resulted in soil self-weight vertical effective stresses at the skirt tip of $\sigma'_v = \gamma' L = 40$ kPa in the centrifuge tests (in sand), compared to $\sigma'_v = 0{\cdot}8$ kPa in the

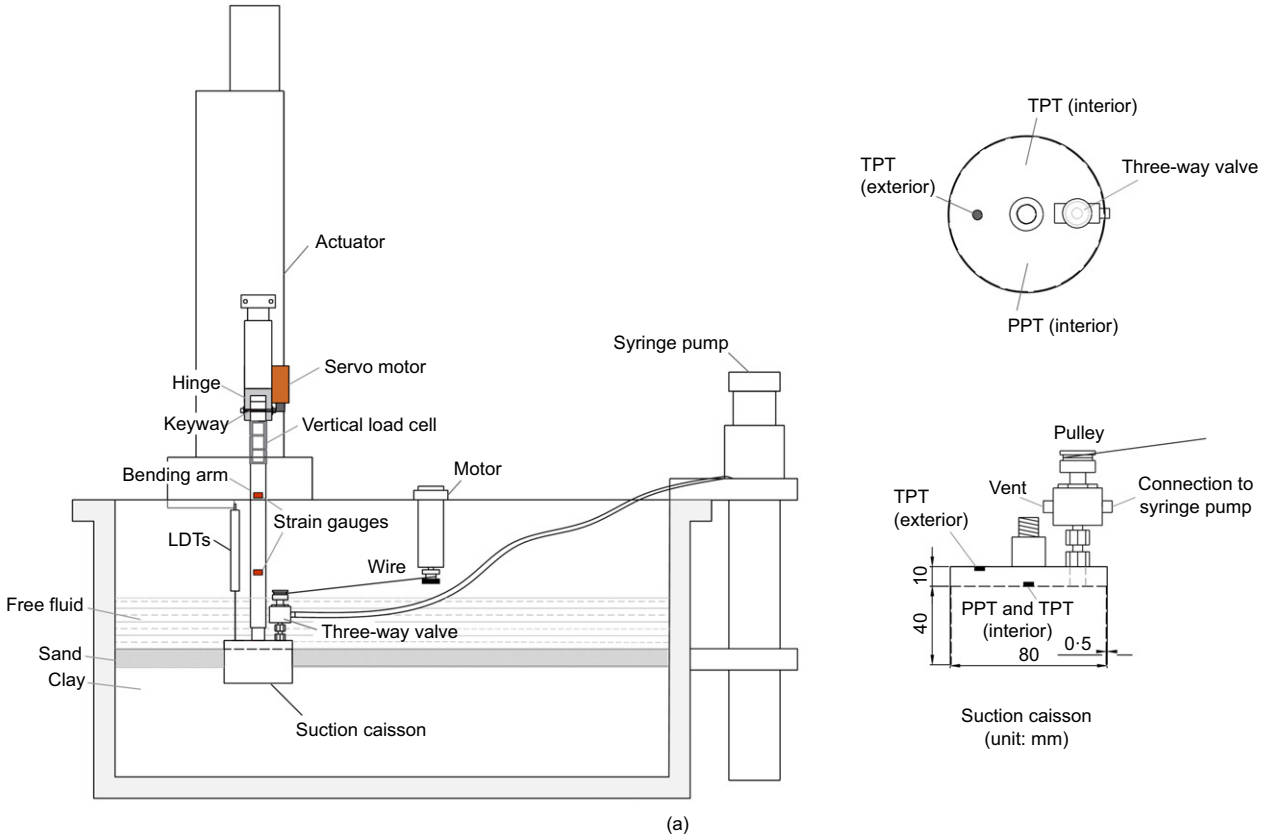

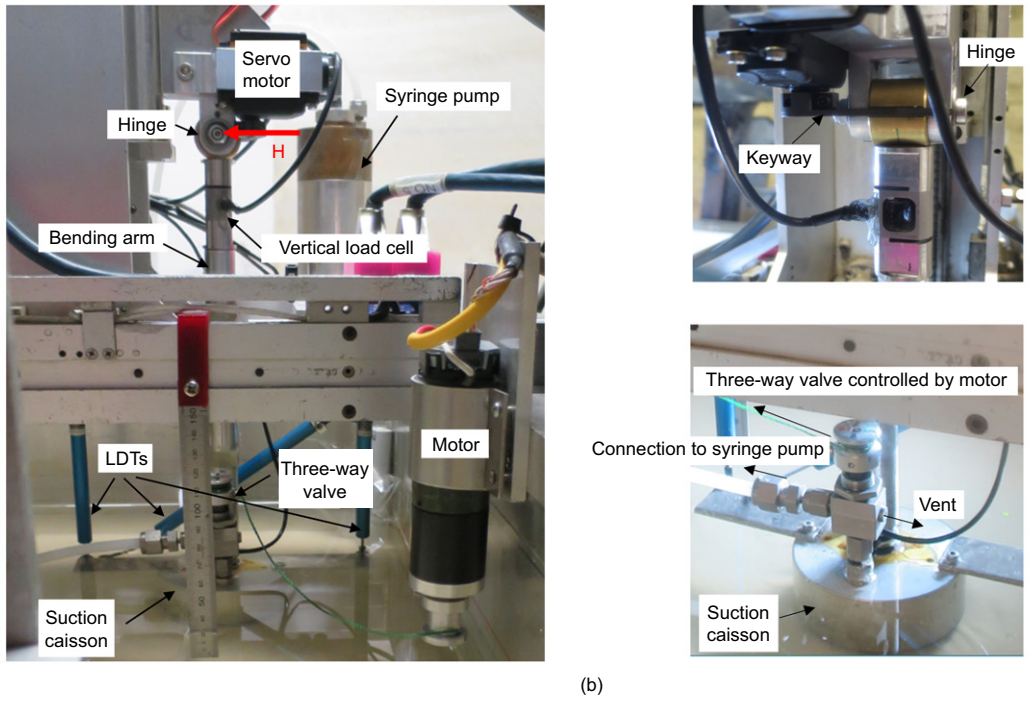

Fig. 1. Experimental arrangement: (a) schematic diagrams; (b) photographs. LDT, linear differential transducer; PPT, pore pressure transducer; TPT, total pressure transducer

corresponding single gravity model scale tests (Zhu *et al.*, 2018). The caisson was installed at the testing acceleration, initially under vertical load control to an applied load of 200 N ($V = 2$ MN in prototype scale) and then by suction using a syringe pump (with recorded installation data in Zhu (2018)). The caisson self-weight was then increased to 350 N ($V = 3{\cdot}5$ MN, modelling the increase in weight due to the wind turbine installation) before applying either a monotonic or cyclic lateral load, H, at a height $3{\cdot}5D$ above the caisson lid invert (Fig. 1). The magnitude of the corresponding dimensionless group is $V/\gamma' D^3 = 0{\cdot}68$ (in sand; $\gamma' = 10$ kN/m^3), which is within the range employed in existing studies: $V/\gamma' D^3 = 0{\cdot}62$ (Zhu *et al.*, 2018), $V/\gamma' D^3 = 0{\cdot}57$ (Zhu *et al.*, 2013), $V/\gamma' D^3 = 0{\cdot}69$ (Cox *et al.*, 2014) and $V/\gamma' D^3 = 0{\cdot}86$ (Foglia *et al.*, 2014), and is within the $V/\gamma' D^3 = 0{\cdot}09$–$0{\cdot}91$ range suggested by Foglia & Ibsen (2016) for field-scale suction caissons supporting offshore wind turbines.

Table 1. Engineering properties of silica sand (after Chow *et al.*, 2015) and kaolin clay (after Stewart, 1992; Richardson *et al.*, 2009)

Silica sand		Kaolin clay	
Specific gravity, G_s	2·65	Specific gravity, G_s	2·60
Mean particle size, d_{50}: mm	0·19	Liquid limit, LL: %	61
Minimum dry density, ρ_{min}: kg/m^3	1461	Plastic limit, PL: %	27
Maximum dry density, ρ_{max}: kg/m^3	1774	Plastic index, I_p: %	34
Critical state friction angle, ϕ'_{cv}: degrees	30	Critical state friction angle ϕ'_{cv}: degrees	23
Coefficient of consolidation, c_v, at $D_r = 83\%$: m^2/year	16 000* $1{\cdot}1 \times 10^7$†	Coefficient of consolidation, c_v, estimated for stress level at skirt tip and OCR = 20: m^2/year	7·5

*When saturated with 700 cSt cellulose ether pore fluid.
†When saturated with 1 cSt water pore fluid.

The sand and clay properties are listed in Table 1. The clay layer was prepared by preconsolidating kaolin slurry to achieve an undrained shear strength, $s_u \approx 80$ kPa. Sand was then pluviated over the clay to a relative density, $D_r = 83\%$, before saturating from the base of the sand layer. Both drained and partially drained behaviour in the sand was modelled by using water as the pore fluid in one sample and a high-viscosity pore fluid (viscosity, $v_c = 700$ cSt) in the remaining two samples. Fig. 2 shows the cone penetration test (CPT) profiles.

RESULTS AND DISCUSSION

The experimental database comprised eight cyclic loading tests to investigate the following effects (Table 2)

(*a*) soil stress level in sand (test 1-2 compared with testing at single gravity)
(*b*) drainage regime in sand (tests 1-2 and 2-1)
(*c*) installation method in sand (tests 2-1 and 2-3)
(*d*) sand over clay (tests 2-3 and 3-3)
(*e*) cyclic load magnitude and symmetry in sand over clay (tests 3-2 to 3-6).

The cyclic load magnitude and symmetry were described using the parameters ζ_b and ζ_c, respectively (LeBlanc *et al.*, 2010)

$$\zeta_b = \frac{M_{max}}{M_{ult}}, \quad \zeta_c = \frac{M_{min}}{M_{max}} \tag{1}$$

where M_{min} and M_{max} are the minimum and maximum moments in a load cycle, and M_{ult} is the ultimate moment capacity obtained from the monotonic tests.

Accumulated rotation

Effects of installation method, stress level and drainage in sand. The accumulation of rotation with cycle number is examined in Fig. 3 for tests in sand with $\zeta_b = 0{\cdot}4$ and $\zeta_c = 0{\cdot}1$. Rotation data are expressed in normalised form, $\Delta\theta(N)/\theta_0 = (\theta_N - \theta_0)/\theta_0$ (LeBlanc *et al.*, 2010), where θ_0 and θ_N are the maximum rotation during first loading to M_{max} and in cycle number N, respectively. The rotation response can be captured by a power law

$$\frac{\Delta\theta(N)}{\theta_0} = \beta \times N^{\alpha} \tag{2}$$

where β quantifies the initial rotation from θ_0 to θ_1 and α quantifies the rate of rotation accumulation with cycle number. The best fit (based on least-squares regression) with the tests on Fig. 3 and other tests in this research was obtained using $\alpha = 0{\cdot}29$, which is comparable with $\alpha = 0{\cdot}31$ for monopiles (LeBlanc *et al.*, 2010; Abadie *et al.*, 2015), $\alpha = 0{\cdot}30$ (Cox *et al.*, 2014) and $\alpha = 0{\cdot}28$ (Zhu *et al.*, 2018) for suction caissons. Zhu *et al.* (2013) report a higher $\alpha = 0{\cdot}39$ for suction caissons in loose dry silty sand, and suction caisson data in dense sand reported by Foglia *et al.* (2014) gave $\alpha = 0{\cdot}18$. Values of θ_0, β and α from this study and previous work are summarised in Table 3. Although the rate of caisson rotation (captured by α) is identical for all tests in this research, the initial rotation when loaded to M_{max} (θ_0) (which reflects the cyclic load magnitude and soil type), and the accumulated rotation after one cycle $\Delta\theta(1) = \theta_1 - \theta_0$ (captured by β) differs for each test. This directly affects the absolute magnitude of accumulated rotation (equation (2)), which is held to strict limits over the design life (e.g. 0·5°; DNV, 2016). The different initial rotation that arises in sand and sand over clay is quantified in Table 3 for different soil self-weight stress levels (i.e. at 1***g*** and ***Ng***), different drainage responses and as a result of the more realistic suction-assisted installation over jacked installation.

The effect of sand permeability and loading rate is emphasised in the centrifuge test data investigating drainage. Full dissipation of excess pore pressures was achieved in less than 30 s in the sand with high-viscosity pore fluid (sample 2) following the step change of lateral load at the end of the test. In the sand saturated with water (sample 1), the dissipation period was too short to be measured, but should be approximately 700 times less than that in sample 2 due to the difference in pore fluid viscosity. This indicates that the accumulated rotation at $N = 1$ (i.e. $\Delta\theta(1) = \theta_0 \times \beta$) is higher (by a factor of approximately four for these tests) when the loading response is drained (in water) than partially drained (in high-viscosity pore fluid), following jacked installation. Jacked installation appears to lead to lower rotation at $N = 1$, which highlights the importance of understanding the effects of the installation process on the soil state. The additional information of initial rotation following jacked installation (tests 1-1 and 2-1) allows the accumulated rotation of suction caissons in sand to be predicted using previously published rates of accumulation (e.g. Cox *et al.*, 2014) as the difference to suction-assisted installation is now known.

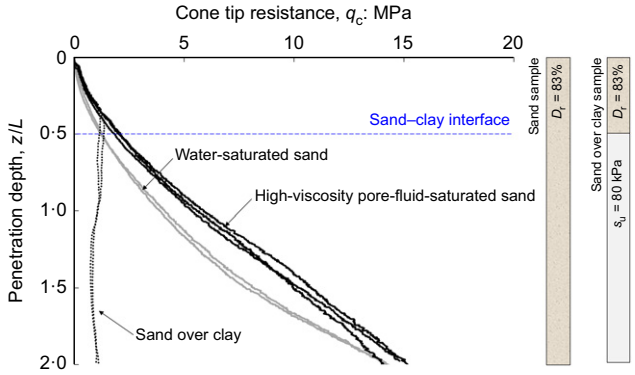

Fig. 2. CPT profiles

Table 2. Centrifuge test programme

Test ID	Soil sample			Installation	Loading type	ζ_b	ζ_c	Cycles, N
	Soil type		Pore fluid					
1-1	Sand	Sand	Water (1 cSt)	Jacked	Monotonic	—	—	—
1-2				Jacked	Cyclic	0·4	0·1	5222
2-1	Sand	Sand	High-viscosity pore fluid (700 cSt)	Jacked	Cyclic	0·4	0·1	547
2-2				Suction	Monotonic	—	—	—
2-3				Suction	Cyclic	0·4	0·1	16 377
3-1	Sand over clay ($H_{sand}/L = 0·5$)	Sand / Clay	High-viscosity pore fluid in sand (700 cSt) Water in clay (1 cSt)	Suction	Monotonic	—	—	—
3-2				Suction	Cyclic	0·7	0·1	2369
3-3				Suction	Cyclic	0·4	0·1	91 793
3-4				Suction	Cyclic	0·4	0·5	4543
3-5				Suction	Cyclic	0·4	−0·7	16 999
3-6				Suction	Cyclic	0·55	0·1	2677

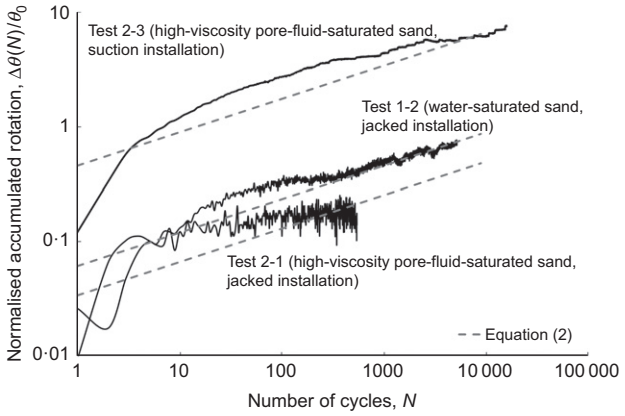

Fig. 3. Effect of installation method on caisson rotation in sand ($\zeta_b = 0·4$, $\zeta_c = 0·1$)

Assessment of the long-term response to cyclic loading requires data over large numbers of cycles. The centrifuge tests are therefore considered collectively with the equivalent single gravity test data reported in Zhu *et al*. (2018) that involved up to one million loading cycles. A comparison in Fig. 4(a) for jacked installation in sand ($\zeta_b = 0·4$, $\zeta_c = 0·1$) shows that the long-term rate of accumulation is almost identical: $\alpha = 0·28$ in the single gravity tests and $\alpha = 0·29$ in the centrifuge tests, although as expected from the preceding discussion, the magnitude of $\Delta\theta(N)/\theta_0$ at $N = 1$ is lower in the single gravity tests ($\beta = 0·06$) than in the centrifuge tests ($\beta = 0·15$). The same rate of accumulated rotation between single gravity and centrifuge tests is also shown to hold for sand over clay ($\zeta_b = 0·4$, $\zeta_c = 0·1$, Fig. 4(b)). These comparisons provide support to an approach of using single gravity tests to assess long-term behaviour, while employing centrifuge tests, involving fewer loading cycles, to quantify the response at relevant stress levels, and where installation and drainage effects are modelled appropriately.

Effect of underlying clay layer. Figure 5 compares $\Delta\theta(N)/\theta_0$ during cyclic loading with $\zeta_b = 0·4$ and $\zeta_c = 0·1$ in sand (test 2-3) to that in sand over clay (test 3-3) following suction installation. Also included in Fig. 5 are fits to the data using equation (2), with $\alpha = 0·29$. The response in the two tests appears broadly similar, although rotation accumulation is initially more rapid in the sand and the rotation eventually stabilises in the sand over clay at $N \approx 10^4$. This stabilisation is not observed in the sand, and although it may be argued that this is due to the lower number of cycles ($N = 16\,377$), equivalent tests in Zhu *et al*. (2018) each with $N \sim 10^6$ show stabilisation in the sand over clay and continuing rotation in the sand. The rotation stabilisation is due to consolidation-induced strength increases in the clay layer, as considered in more detail later. Although the magnitude of $\Delta\theta(N)/\theta_0$ is similar in the sand and the sand over clay, the absolute rotation is slightly higher in the sand over clay profile considered here, as shown by the inset figure.

Effect of cyclic load magnitude and symmetry. Figure 6 allows for an examination of the effect of cyclic load symmetry ($\zeta_c = 0·5$, 0·1 and −0·7 at constant cyclic load magnitude, $\zeta_b = 0·4$, Fig. 6(a)) and magnitude ($\zeta_b = 0·4$, 0·55 and 0·7 at a fixed one-way load symmetry, $\zeta_c = 0·1$, Fig. 6(b)) on rotation accumulation in sand over clay. Fig. 6(a) shows that the normalised accumulated rotation, $\Delta\theta(N)/\theta_0$, is similar for both one-way cyclic loading cases considered ($\zeta_c = 0·5$ and 0·1) and larger than that under two-way cyclic loading ($\zeta_c = -0·7$). The normalised rotation, $\Delta\theta(N)/\theta_0$, is similar and accumulates with cycle number at the same rate ($\alpha = 0·29$; the stabilised rotation observed in some of the tests was not included in the regression analysis to obtain α and β), but as shown by the inset figure, the absolute rotation, θ_N, increases with ζ_b. The increase is apparent by the first cycle indicating that the rotation simply increases with load magnitude during the initial loading to M_{max}. The above trends are consistent with the observations of Zhu *et al*. (2018) from single gravity tests in the same soil profile ($H_{sand}/L = 0·5$) where the caisson was installed by jacking and water was used as the pore fluid.

The rotation in test 3-3 (in sand over clay) stabilised at about $N = 10^4$. Similar behaviour is also apparent in test 3-5, although the effect is not as prominent due to the lower number of cycles involved in this test ($N = 16\,999$). As similar behaviour was not observed in the sand samples, this stabilising response must be due to strength changes in the clay layer. Supporting evidence is provided in Fig. 7, which plots the pore pressure response for test 3-3 and test 3-5. Approximately 90% of the excess pore pressure (measured at the caisson lid invert) is dissipated by $N = 10^4$, which is approximately the same point at which the rotation stabilised. This consolidation will cause a strength increase in the clay, which will limit the rotation. Also shown in Fig. 7 is the corresponding pore pressure response for test 2-3 in sand (saturated with the high-viscosity pore fluid), where the pore pressure, Δu, is normalised by the average maximum pore pressure, Δu_i, measured in the sand over clay tests. Accumulation of pore pressures during cyclic loading in sand is negligible compared with that in sand over clay.

Table 3. Fitted α and β from tests in sand and sand over clay ($H_{sand}/L = 0{\cdot}5$)

α	β	N	θ_0	Soil type	Install.	Pore fluid in sand	ζ_b	ζ_c	Approach	Source
0·18	0·53	$\sim 10^4$	*	Sand	Jacked	Water	0·4	−0·05	1*g*	Foglia *et al.* (2014)†
0·39	0·10	10 325	*	Sand	Jacked	Dry sand	0·37	0	1*g*	Zhu *et al.* (2013)†
0·30	0·10	71	*	Sand	Jacked	Dry sand	0·4	0·02	*Ng*	Cox *et al.* (2014)†
0·28	0·15 ± 0·03	1 204 998	0·017°	Sand	Jacked	Water	0·4	0·1	1*g*	Zhu *et al.* (2018)†
0·29	0·06	5222	0·013°	Sand	Jacked	Water	0·4	0·1	*Ng*	Present study, test 1-2
	0·03	547	0·006°	Sand	Jacked	High-viscosity pore fluid	0·4	0·1	*Ng*	Present study, test 2-1
	0·45	16 377	0·013°	Sand	Suction	High-viscosity pore fluid	0·4	0·1	*Ng*	Present study, test 2-3
	0·67	91 793	0·029°	Sand over clay	Suction	High-viscosity pore fluid	0·4	0·1	*Ng*	Present study, test 3-3
	0·62	4543	0·035°	Sand over clay	Suction	High-viscosity pore fluid	0·4	0·5	*Ng*	Present study, test 3-4
	0·17	16 999	0·032°	Sand over clay	Suction	High-viscosity pore fluid	0·4	−0·7	*Ng*	Present study, test 3-5
	0·52	2677	0·042°	Sand over clay	Suction	High-viscosity pore fluid	0·55	0·1	*Ng*	Present study, test 3-6
	0·29	2369	0·286°	Sand over clay	Suction	High-viscosity pore fluid	0·7	0·1	*Ng*	Present study, test 3-1

*Not known.
†Only data for $\zeta_b \approx 0{\cdot}4$ and $\zeta_c \approx 0{\cdot}1$ are provided here. Parameters relevant to other values of ζ_b and ζ_c can be found in the original studies.

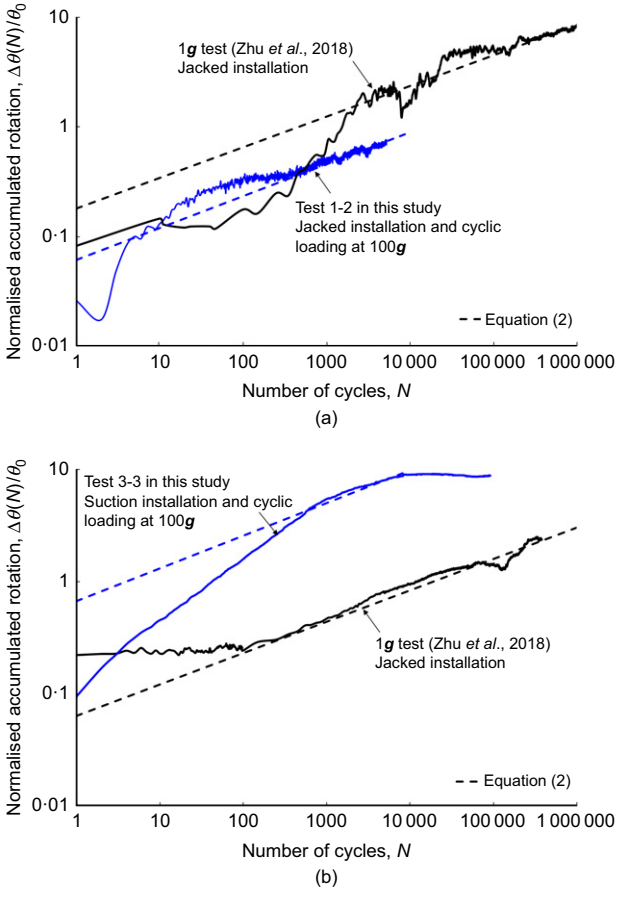

Fig. 4. Accumulated caisson rotation for: (a) jacked installation in fully drained sand; (b) sand over clay following jacked installation in single gravity test (Zhu *et al.*, 2018) and suction installation in test 3-3 of this centrifuge study ($\zeta_b = 0{\cdot}4$, $\zeta_c = 0{\cdot}1$)

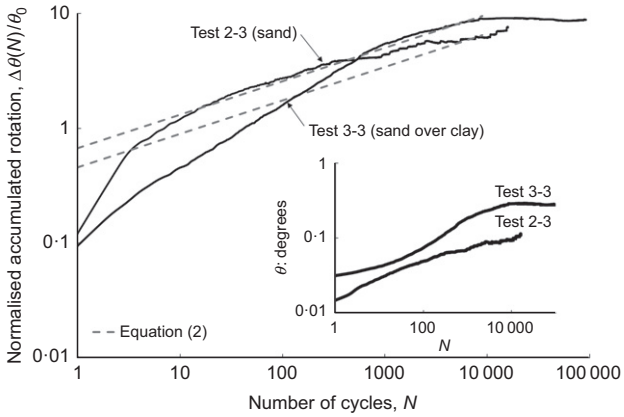

Fig. 5. Effect of an underlying clay layer on accumulation of caisson rotation during cyclic loading with $\zeta_b = 0{\cdot}4$ and $\zeta_c = 0{\cdot}1$

Figures 6 and 7 also include the dimensionless time $T = c_v t/D^2$ as secondary horizontal axes (where t is the time since the onset of cyclic loading and c_v is the coefficient of consolidation of the clay, which will dominate the drainage response). The use of T (applicable to the sand over clay results) permits assessment of consolidation for other caisson dimensions and soil properties. For example, caisson rotation stabilises in the sand over clay tests at $T \approx 0{\cdot}7$, which for the prototype equivalent of the caisson and soils used in these centrifuge experiments, corresponds to a duration of approximately 6 years.

Application to field conditions. Applying equation (2) to the prototype caisson geometry and soil properties considered in these tests would result in 0·3° of rotation for two-way loading ($\zeta_c = -0{\cdot}7$) and 1·1° of rotation for one-way loading ($\zeta_c = 0{\cdot}1$) for a load magnitude, $\zeta_b = 0{\cdot}4$ and one million loading cycles. On the basis of this simple calculation, the one-way loading would exceed the DNV (2016) rotation limit of 0·5°, although this conservative estimate neglects the stabilising effect from consolidation in the clay. In contrast the same calculations for a one-way loading scenario in sand would lead to a more moderate rotation of 0·3° (i.e. using $\beta = 0{\cdot}45$ and $\theta_0 = 0{\cdot}013°$).

Unloading stiffness

This section examines the effect of cyclic loading on unloading stiffness, k, determined from the maximum

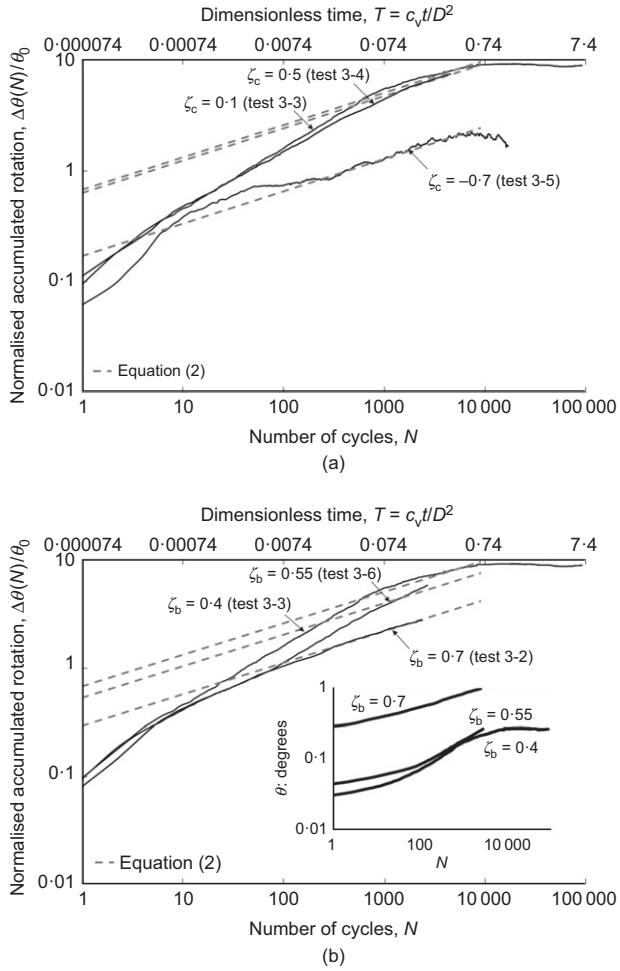

Fig. 6. Accumulated rotation with number of loading cycles for tests in sand over clay: (a) $\zeta_b = 0{\cdot}4$ with $\zeta_c = 0{\cdot}5$, 0·1 and −0·7; (b) $\zeta_c = 0{\cdot}1$ with $\zeta_b = 0{\cdot}4$, 0·55 and 0·7

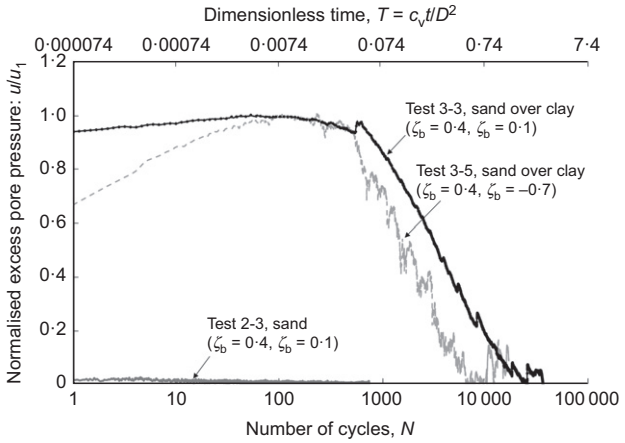

Fig. 7. Pore-pressure response during cyclic loading in sand over clay

and minimum loads and rotations in cycle N relative to that in the first cycle and expressed as k_N/k_1, as illustrated in Fig. 8.

Stiffness in sand. The evolution of k_N/k_1 (Fig. 9) in sand is similar over the initial ten cycles, and the test results most relevant to field conditions (with high-viscosity pore fluid) exhibit a steady but moderate 20–50% increase in

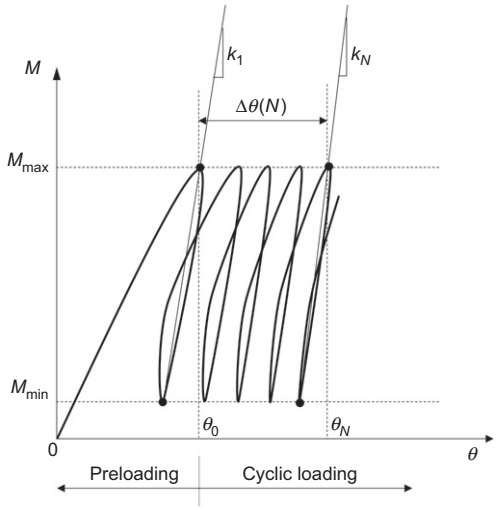

Fig. 8. Definition of accumulated rotation and stiffness (after LeBlanc *et al.*, 2010)

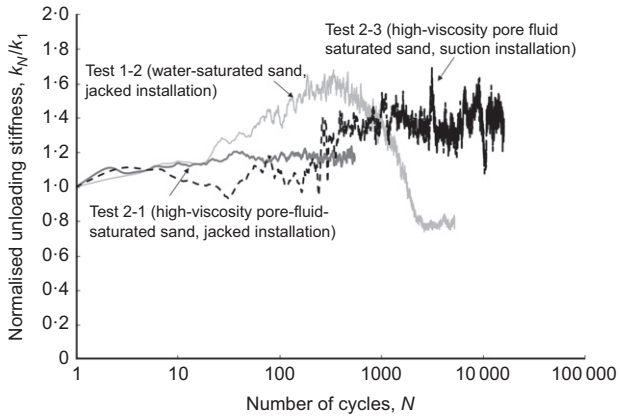

Fig. 9. Evolution of unloading stiffness with number of loading cycles in sand ($\zeta_b = 0{\cdot}4$, $\zeta_c = 0{\cdot}1$) with different pore fluids and installation methods

stiffness throughout. The stiffness ratio in the jacked test in water-saturated sand increases to $k_N/k_1 = 1{\cdot}6$ before showing a drop, consistent with observations from single gravity tests (Zhu *et al.*, 2018). This drop is not evident following suction installation.

Stiffness in sand over clay. In sand over clay (Fig. 10(a)), tests involving one-way loading ($\zeta_c \geq 0$) at relatively low load magnitudes ($\zeta_b = 0{\cdot}4$) show a reduction in unloading stiffness that (partially) recovers over the duration of the test. In contrast, the low load magnitude two-way cyclic loading test ($\zeta_c = -0{\cdot}7$, $\zeta_b = 0{\cdot}4$) and the one-way cyclic loading test at a higher load magnitude ($\zeta_c = 0{\cdot}5$, $\zeta_b = 0{\cdot}7$) show little change in stiffness but then start to increase, moderately at first, but more rapidly at $N \approx 5000$ in test 3-5, which reaches $k_N/k_1 \approx 2{\cdot}75$ after $N \approx 10\,000$. The point at which the stiffness starts to increase ($N \approx 200$) appears to be consistent with when the pore pressure measured at the lid invert starts to reduce (see Fig. 7). The more rapid increase in stiffness observed at $N \approx 5000$ in test 3-5 coincides with when pore pressure dissipation is near complete (Fig. 7), which leads to stabilisation of the rotation and hence a rapid increase in stiffness. Comparisons with equivalent single gravity tests (Fig. 10(b)) show that the stiffness increase is more moderate

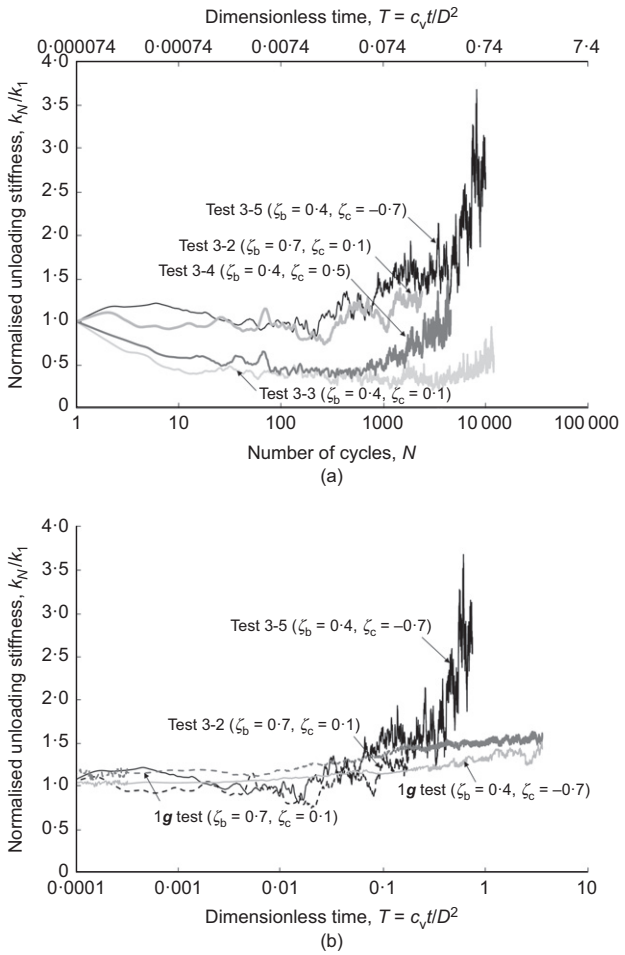

Fig. 10. Evolution of unloading stiffness with number of loading cycles in sand over clay: (a) with different cyclic load magnitude and symmetry (ζ_b and ζ_c); (b) compared with long-term data reported in Zhu *et al.* (2018)

and steady in the long term. The disparity may be due to soil self-weight stress level effects and warrants further attention given the potential for stiffness changes to affect system dynamics.

CONCLUSIONS

This note discusses the response of a suction caisson subjected to lateral cyclic loads on the basis of collective consideration of single gravity and centrifuge test results. The centrifuge tests model the correct soil self-weight stress levels, installation process and drainage response but could only test on the order of 10^4 cycles. This note has shown that for the conditions within this study, these accurate post-installation centrifuge measurements can be combined with the results from single gravity model tests on significantly more cycles to predict the long-term serviceability response of a suction caisson under lateral cyclic loading, with the accumulation of caisson rotation captured by a simple calculation approach. Application of this calculation approach to field conditions showed that the long-term rotation for one-way loading would be higher for a sand over clay seabed than for a sand seabed. Evidently the validity of this finding needs to be established beyond the parameter base considered in these model tests. Beneficial effects from densification of sand and consolidation in the clay lead to stiffness increases – the effect of these increases on the natural frequency of the offshore wind turbine needs to be considered in design.

ACKNOWLEDGEMENTS

This work forms part of the activities of COFS, which is currently supported as one of the primary nodes of the Australian Research Council Centre of Excellence for Geotechnical Science and Engineering and as a Centre of Excellence by the Lloyd's Register Foundation. Lloyd's Register Foundation helps to protect life and property by supporting engineering-related education, public engagement and the application of research. The project also received funding from Lloyd's Register. John Breen, Guido Wager, Khin Thida Seint, Manuel Palacios, Kelvin Leong and Dave Jones provided assistance during the tests. The above support is gratefully appreciated.

NOTATION

c_v	coefficient of vertical consolidation
D	caisson diameter
D_r	relative density
e	eccentricity of lateral load
H	lateral load
H_{sand}	sand layer thickness
k	unloading stiffness
k_1	unloading stiffness in the first cycle
k_N	unloading stiffness in cycle number N
L	skirt length
M	overturning moment
M_{max}	maximum moment in a load cycle
M_{min}	minimum moment in a load cycle
M_{ult}	ultimate moment capacity
N	number of cycles
q_c	cone tip resistance
s_u	undrained shear strength
T	dimensionless time
t	skirt thickness, time
z	penetration depth
α	dimensionless variable
β	dimensionless variable
γ'	effective unit weight of soil
Δu	change in excess pore pressure
Δu_i	maximum excess pore pressure
$\Delta\theta(N)$	accumulated rotation during cyclic loading
ζ_b	parameter describing cyclic loading magnitude
ζ_c	parameter describing cyclic loading symmetry
θ	caisson rotation
θ_0	maximum rotation during preloading to M_{max}
θ_N	maximum rotation in cycle number N
ν_w	viscosity of water
ν_c	viscosity of cellulose ether fluid
σ'_v	vertical effective stress

REFERENCES

Abadie, C. N., Byrne, B. W. & Levy-Paing, S. (2015). Model pile response to multi-amplitude cyclic lateral loading in cohesionless soils. In *Proceedings of the 3rd international symposium on frontiers in offshore geotechnics (ISFOG)* (ed. V. Meyer), pp. 681–686. Leiden, the Netherlands: CRC Press/Balkema (Taylor & Francis Group).

BGS (British Geological Survey) (2002). *North Sea geology*, Technical report produced for strategic environmental assessment – SEA2 and SEA3 (TR_008). Nottingham, UK: BGS. See https://www.gov.uk/government/uploads/system/uploads/attachment_data/file/197347/TR_SEA3_Geology.pdf (accessed 19/11/2018).

Bhattacharya, S. (2014). *Challenges in design of foundations for offshore wind turbines*, Engineering and Technology Reference. Stevenage, UK: Institution of Engineering and Technology (IET).

Bienen, B., O'Loughlin, C. D. & Zhu, F. Y. (2017). Physical modelling of suction bucket installation and response under long-term cyclic loading. In *Proceedings of 8th offshore site investigation and geotechnics international conference (OSIG*

2017), pp. 524–531. London, UK: Society for Underwater Technology.

Bond, A. J., Hight, D. W. & Jardine, R. J. (1997). *Design of piles in sand in the UK sector of the North Sea*. Liverpool, UK: Health & Safety Executive, HSE Books.

Cox, J. A., O'Loughlin, C. D., Cassidy, M., Bhattacharya, S., Gaudin, C. & Bienen, B. (2014). Centrifuge study on the cyclic performance of caissons in sand. *Int. J. Phys. Modelling Geotech.* **14**, No. 4, 99–115.

Chow, S. H., O'Loughlin, C. D., Corti, R., Gaudin, C. & Diambra, A. (2015). Drained cyclic capacity of plate anchors in dense sand: experimental and theoretical observations. *Géotechnique Lett.* **5**, No. 2, 80–85, https://doi.org/10.1680/geolett.15.00019.

De Ruiter, J. & Fox, D. A. (1975). Site investigations for North Sea forties field. *Proceedings of the 7th annual offshore technology conference (OTC)*, Houston, TX, USA, OCT 2246, pp. 25–30.

DNV (Det Norske Veritas) (2016). *Support structures for wind turbines. Offshore standard (DNVGL-ST-0126)*. Oslo, Norway: DNV.

Foglia, A. & Ibsen, L. B. (2016). Monopod bucket foundations under cyclic lateral loading. *Int. J. Offshore Polar Engng* **26**, No. 2, 109–115.

Foglia, A., Ibsen, L. B., Nicolai, G. & Andersen, L. V. (2014). Observations on bucket foundations under cyclic loading in dense saturated sand. In *Proceedings of the 8th international conference of physical modelling in geotechnics (ICPMG)* (eds C. Gaudin and D. J. White), pp. 667–673. Leiden, the Netherlands: CRC Press/Balkema (Taylor & Francis Group).

LeBlanc, C., Houlsby, G. T. & Byrne, B. W. (2010). Response of stiff piles in sand to long-term cyclic lateral loading. *Géotechnique* **60**, No. 2, 70–90, https://doi.org/10.1680/geot.7.00196.

Richardson, M. D., O'Loughlin, C. D., Randolph, M. F. & Gaudin, C. (2009). Setup following installation of dynamic anchors in normally consolidated clay. *J. Geotech. Geoenviron. Engng* **135**, No. 4, 487–496.

Stewart, D. P. (1992). *Lateral loading of piled bridge abutments due to embankment construction*. PhD thesis, The University of Western Australia, Perth, Australia.

Zhu, F. Y. (2018). *Suction caisson foundations for offshore wind energy installations in layered soils*. PhD thesis, The University of Western Australia, Crawley, Perth, Australia.

Zhu, B., Byrne, B. W. & Houlsby, G. T. (2013). Long-term lateral cyclic response of suction caisson foundations in sand. *J. Geotech. Geoenviron. Engng* **139**, No. 1, 73–83.

Zhu, F. Y., O'Loughlin, C., Bienen, B., Cassidy, M. J. & Morgan, N. (2018). The response of suction caissons to long-term lateral cyclic loading in single-layer and layered seabeds. *Géotechnique* **68**, No. 8, 729–741, https://doi.org/10.1680/jgeot.17.P.129.